Radioluminescence in Al_2O_3 : C – analytical and numerical simulation results

2009 J. Phys. D: Appl. Phys. 42 175107

(http://iopscience.iop.org/0022-3727/42/17/175107)

IOP PUBLISHING JOURNAL OF PHYSICS D: APPLIED PHYSICS

J. Phys. D: Appl. Phys. **42** (2009) 175107 (9pp) doi:10.1088/0022-3727/42/17/175107

Radioluminescence in Al_2O_3 : C – analytical and numerical simulation results

V Pagonis[1,5], J Lawless[2], R Chen[3] and C Andersen[4]

[1] Physics Department, McDaniel College, Westminster, MD 21157, USA
[2] Redwood Scientific Inc., Pacifica, CA 94044, USA
[3] Raymond and Beverly Sackler School of Physics and Astronomy, Tel-Aviv University, Tel-Aviv 69978, Israel
[4] Risø National Laboratory, Radiation Research Department, DK-4000 Roskilde, Denmark

E-mail: vpagonis@mcdaniel.edu

Received 12 May 2009, in final form 22 July 2009
Published 20 August 2009
Online at stacks.iop.org/JPhysD/42/175107

Abstract

The phenomenon of radioluminescence (RL) has been reported in a number of materials including Al_2O_3 : C, which is one of the main dosimetric materials. In this work, we study RL using a kinetic model involving two trapping states and two kinds of recombination centres. The model has been previously used to provide a quantitative description of the thermoluminescence and optically stimulated luminescence processes in Al_2O_3 : C. Using appropriate sets of trapping parameters for the kinetic model, the RL signal along with the occupancies of the relevant traps and centres are simulated numerically. The set of differential equations is also solved analytically by assuming dynamic balance during sample irradiation. Analytical expressions are obtained for the concentrations of traps and centres in the material during irradiation with short irradiation pulses, by assuming that quasi-steady conditions hold during irradiation. Several experimentally observed characteristics of the RL signals are explained by using the model. Good quantitative agreement is found between the analytical expressions and the numerical solutions of the model for short irradiation pulses.

1. Introduction

Over the last decade attention has been given to applications of the dosimetric material Al_2O_3 : C in medical dosimetry. One such application is *in vivo* dose verification in radiotherapy of cancer patients. Andersen *et al* [1] have developed a system for *in vivo* dose measurements during radiotherapy. Their system uses the radioluminescence (RL) and optically stimulated luminescence (OSL) signals from small Al_2O_3 : C crystals attached to long optical fibre cables. During radiation therapy, the RL signal provides a real-time measurement of the dose rate at the position of the crystal, and immediately after the treatment, the continuous wave (CW) OSL signal is used to determine the integrated dose (see, for example, Aznar *et al* [2]).

These experimental studies have established several empirical results for RL measurements carried out in Al_2O_3 : C crystals. Three such important results are shown in figure 1, which reproduces experimental data from Aznar [3], figure 3.9, page 43. Specifically, figure 1(*a*) shows that the RL intensity during a short irradiation pulse increases linearly with time. The experimental data in figure 1(*b*) indicate that the corresponding initial RL intensity I_o varies linearly with the dose rate X, while figure 1(*c*) demonstrates that the slope of the linear part of the RL intensity varies quadratically with the dose rate X. The results shown in figure 1(*a*)–(*c*) are mostly empirical in nature, and no analytical expressions have been previously offered in the literature.

In this work, we study the RL signal from Al_2O_3 : C by using a kinetic model consisting of two trapping states and two kinds of recombination centres. This model has been previously used successfully to provide a quantitative description of the dose response of thermoluminescence (TL), OSL and UV-induced TL signals from Al_2O_3 : C crystals (see, for example, Chen *et al* [4], Pagonis *et al* [5], Pagonis *et al* [6]).

In this paper the RL signal during irradiation of Al_2O_3 : C samples is simulated numerically, along with the occupancies

[5] Author to whom any correspondence should be addressed.

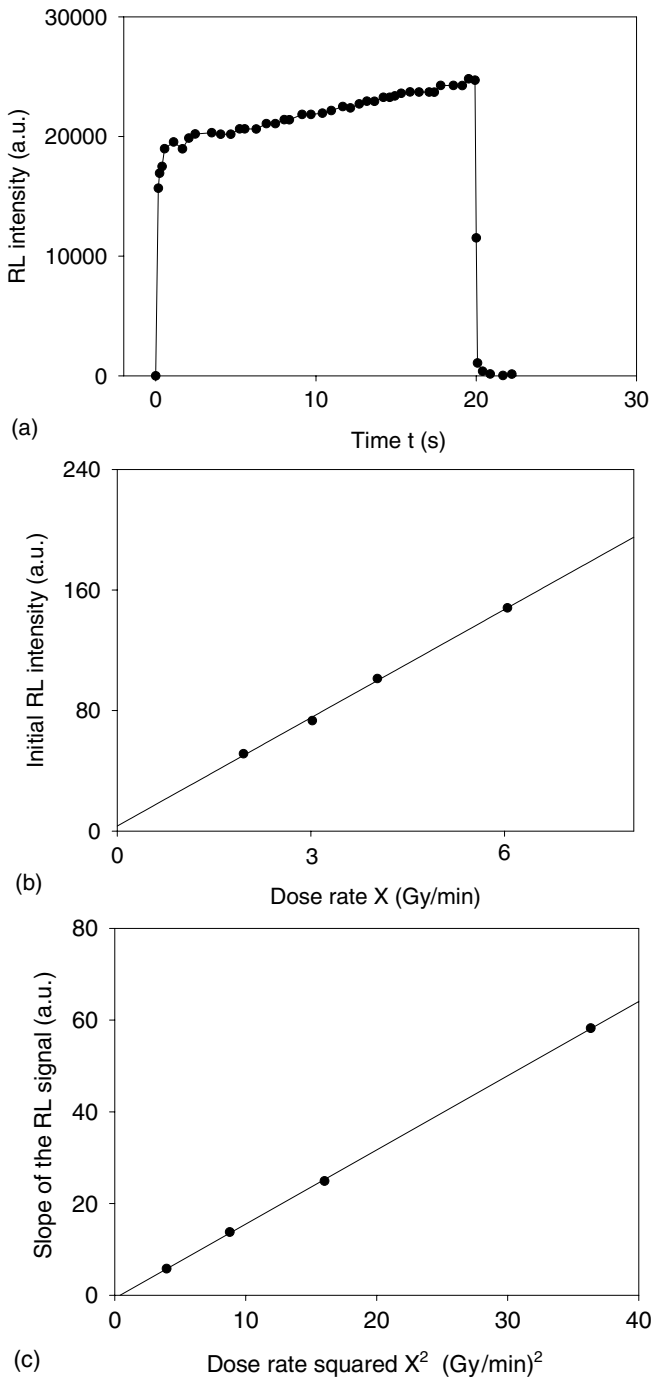

Figure 1. Previous experimental results obtained by Aznar [3] during RL experiments on $Al_2O_3:C$ samples are redrawn here for reference purposes. (*a*) The RL pulses as a function of time are characterized by a linear region. (*b*) The initial RL intensity I_o of the RL pulses in (*a*) is found empirically to depend linearly on the dose rate X. (*c*) The slope of the RL pulses shown in (*a*) is found empirically to depend linearly on the square of the dose rate X^2 used during the RL experiments.

of the relevant traps and centres. The set of differential equations is also solved analytically by assuming dynamic balance during sample irradiation, and analytical expressions are obtained for the concentrations of traps and centres during short irradiation pulses. The empirical characteristics of the RL signal shown in figure 1 are explained by using the results of the model.

2. The model

The model presented in this section has some similarities to previously published kinetic models for the RL phenomenon in $Al_2O_3:C$ and feldspars [7–15]. The schematic details of the model are shown in figure 2, and it is identical to the model used by Pagonis *et al* (2007) to explain the dose response of the TL dose signal from $Al_2O_3:C$. In Pagonis *et al* [5] the model was used to fit the experimental data of Yukihara *et al* [9] for three different samples labelled Chip101, D320 and B1040.

Two electron trapping states are taken into consideration in the model, N_1 which is the main dosimetric trap from which stimulating light can release electrons, and N_2, a competitor in which electrons can be trapped, but the stimulating light cannot release electrons from it. Two recombination centres are assumed to exist, M_1 which is radiative and M_2, a non-radiative competitor. The various transitions in the model taking place during an RL measurement are indicated by arrows in figure 2. The set of six coupled differential equations governing the process during excitation is

$$\frac{dm_1}{dt} = -A_{m1}m_1n_c + B_1(M_1 - m_1)n_v, \tag{1}$$

$$\frac{dm_2}{dt} = -A_{m2}m_2n_c + B_2(M_2 - m_2)n_v, \tag{2}$$

$$\frac{dn_1}{dt} = A_{n1}(N_1 - n_1)n_c, \tag{3}$$

$$\frac{dn_2}{dt} = A_{n2}(N_2 - n_2)n_c, \tag{4}$$

$$\frac{dn_v}{dt} = X - B_2(M_2 - m_2)n_v - B_1(M_1 - m_1)n_v, \tag{5}$$

$$\frac{dn_c}{dt} = X - A_{n1}(N_1 - n_1)n_c - A_{n2}(N_2 - n_2)n_c - A_{m1}m_1n_c - A_{m2}m_2n_c, \tag{6}$$

where M_2 (cm^{-3}) is the concentration of non-radiative hole centres with instantaneous occupancy of m_2 (cm^{-3}), M_1 (cm^{-3}) is the concentration of radiative hole centres with instantaneous occupancy of m_1 (cm^{-3}), N_1 (cm^{-3}) is the concentration of the electron active dosimetric trap with instantaneous occupancy of n_1 (cm^{-3}) and N_2 (cm^{-3}) is the concentration of the competitor trapping state with instantaneous occupancy of n_2 (cm^{-3}). n_c and n_v are the concentrations (cm^{-3}) of the electrons and holes in the conduction band (CB) and valence band (VB), respectively. X ($cm^{-3}\,s^{-1}$) is the rate of production of electron–hole pairs, which is proportional to the excitation dose rate, B_1 and B_2 ($cm^3\,s^{-1}$) are the trapping probability coefficients of free holes in centres 1 and 2, respectively. A_{m1} and A_{m2} ($cm^3\,s^{-1}$) are the recombination probability coefficients for free electrons with holes in centres 1 and 2, and A_{n1} ($cm^3\,s^{-1}$) is the retrapping probability coefficient of free electrons into the active trapping state N_1. A_{n2} ($cm^3\,s^{-1}$) is the retrapping probability coefficient of the free electrons into the competing trapping state N_2. If we denote the time of excitation by t_D and the rate of production of electron–hole pairs per cm^3 per second by X, then $X \times t_D$ represents the total concentration of electrons and

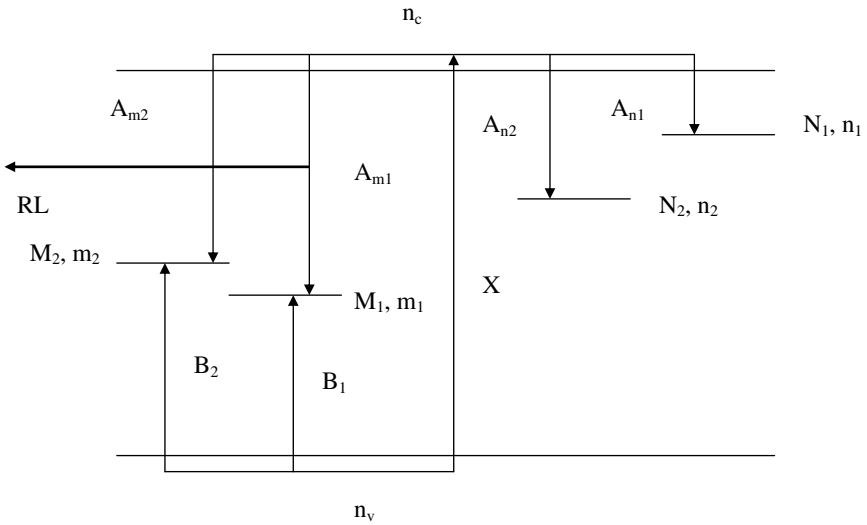

Figure 2. The energy level diagram of two electron trapping states and two kinds of hole recombination centres. Transitions occurring during irradiation of the sample are given by solid lines.

holes produced, which is proportional to the total dose imparted on the sample.

The RL intensity is associated with the recombination into m_1; therefore, the intensity $I(t)$ is given by

$$I(t) = A_{m1} m_1 n_c. \tag{7}$$

In the rest of this section we present an analytical solution to the system of equations (1)–(7). The only assumptions used during this derivation are that the quasi-steady conditions hold and that the initial concentrations of electrons and holes in the model are $m_1(0) = m_{10}$ and $n_{10} = n_{20} = m_{20} = 0$. Experimentally it is possible to achieve these initial conditions by annealing the material at a high temperature, as is commonly done before using a dosimetric material.

After a very short transitional period, a dynamic balance is established between the irradiation process creating pairs of electrons and holes on the one hand, and the relaxation process of electrons and holes into the various energy levels on the other. According to the quasi-static assumption commonly made in kinetic models, we can assume that during this dynamic balance the concentrations of electrons in the CB and of holes in the VB change very slowly, so that $dn_v/dt = 0$ and $dn_c/dt = 0$. By substituting $dn_v/dt \approx 0$ into equation (5), it can be solved for n_v to yield

$$n_v = \frac{X}{B_2(M_2 - m_2) + B_1(M_1 - m_1)}. \tag{8}$$

The initial concentration n_{v0} of holes in the VB at time $t = 0$ can be obtained by replacing the concentrations m_1 and m_2 in equation (8) with their initial values at time $t = 0$, i.e. $m_2 = m_{20} = 0$ and $m_1 = m_{10}$. Equation (8) then yields

$$n_{v0} = \frac{X}{B_2 M_2 + B_1(M_1 - m_{10})}. \tag{9}$$

In a similar manner by assuming that during dynamic balance $dn_c/dt = 0$ equation (6) can be solved for n_c to yield

$$n_c = \frac{X}{A_{n1}(N_1 - n_1) + A_{n2}(N_2 - n_2) + A_{m1} m_1 + A_{m2} m_2}. \tag{10}$$

The initial concentration n_{c0} of electrons in the CB at time $t = 0$ is obtained by replacing the concentrations n_1, n_2, m_1 and m_2 with their initial concentrations in equation (10) to obtain

$$n_{c0} = \frac{X}{A_{n1} N_1 + A_{n2} N_2 + A_{m1} m_{10}}. \tag{11}$$

For short irradiation pulses the RL intensity $I(t)$ can be expanded as a Taylor series about $t = 0$. Our goal is to find the first two terms of the series expansion:

$$I(t) = C_1 + C_2 t + O(t^2), \tag{12}$$

with the coefficients C_1 and C_2 given by

$$C_1 = I(0), \tag{13}$$

$$C_2 = \left.\frac{dI(t)}{dt}\right|_{t=0}. \tag{14}$$

The calculation of C_1 is straightforward by using equation (7) for $I(t)$ and equation (11) for the initial quasi-steady equilibrium value of n_{c0}:

$$C_1 = I(0) = A_{m1} m_{10} n_{c0} = \frac{A_{m1} m_{10} X}{A_{n1} N_1 + A_{n2} N_2 + A_{m1} m_{10}}. \tag{15}$$

From equations (13) and (15) we see that the constant C_1 represents the initial RL intensity I_o at $t \sim 0$ and hence the initial RL intensity is equal to

$$I_o = C_1 = \frac{A_{m1} m_{10} X}{A_{n1} N_1 + A_{n2} N_2 + A_{m1} m_{10}}. \tag{16}$$

Equation (16) indicates that the initial RL intensity I_o will be proportional to the dose rate X used during the RL experiment, in agreement with the empirical data shown in figure 1(*b*).

The calculation of the constant coefficient C_2 in equation (12) is more complex algebraically, and is derived

in detail in appendix A. The result after much algebra is

$$C_2 = \frac{A_{m1}X^2}{(A_{n1}N_1 + A_{n2}N_2 + A_{m1}m_{10})^2} \times \left(m_{10}\frac{A_{n1}^2N_1 + A_{n2}^2N_2 - A_{m1}(A_{n1}N_1 + A_{n2}N_2)}{A_{n1}N_1 + A_{n2}N_2 + A_{m1}m_{10}} + \frac{(A_{n1}N_1 + A_{n2}N_2)B_1(M_1 - m_{10}) - A_{m2}B_2M_2m_{10}}{B_1(M_1 - m_{10}) + B_2M_2} \right). \quad (17)$$

Equations (12) and (17) show that for a constant dose rate X the RL intensity will be increasing linearly with time t, in agreement with the empirical data shown in figure 1(*a*). The slope of this linear dependence of $I(t)$ is given by the constant C_2:

$$\text{slope of } I(t) = C_2. \quad (18)$$

Equations (17) and (18) indicate that the slope of the linear part of the RL signal $I(t)$ should be proportional to the square of the dose rate X^2. This prediction from the model is in agreement with the empirical data shown in figure 1(*c*).

It is emphasized that the derivation of C_1 and C_2 in equations (15) and (17) is based solely on the validity of the quasi-steady conditions, and uses no other approximations.

We can also obtain analytical expressions for the electron and hole concentrations $m_1(t), n_1(t), n_2(t), m_2(t)$ as shown in detail in appendix B. By substituting equations (9) and (11) in the differential equations (1)–(4) and carrying out the integrations of the first order differential equations, the following approximate analytical expressions for the concentrations m_1 , m_2 , n_1 and n_2 are obtained in appendix B:

$$n_1(t) = N_1\left(1 - \exp\left(-\frac{A_{n1}Xt}{A_{n2}N_2 + A_{n1}N_1 + A_{m1}m_{10}}\right)\right), \quad (19)$$

$$n_2(t) = N_2\left(1 - \exp\left(-\frac{A_{n2}Xt}{A_{n2}N_2 + A_{n1}N_1 + A_{m1}m_{10}}\right)\right), \quad (20)$$

$$m_1(t) = \left[A_{m1}m_{10}(B_1M_1 + B_2M_2e^{-DtX}) + B_1(M_1(1 - e^{-DtX}) + m_{10})(A_{n1}N_1 + A_{n2}N_2)\right] \times \left[A_{m1}B_1M_1 + A_{m1}B_2M_2 + A_{n1}B_1N_1 + A_{n2}B_1N_2\right]^{-1}, \quad (21)$$

$$m_2(t) = \left[B_2M_2(1 - e^{-EtX})(A_{n1}N_1 + A_{n2}N_2 + A_{m1}m_{10})\right] \times \left[A_{m2}(B_1M_1 - B_1m_{10} + B_2M_2) + B_2(A_{m1}m_{10} + A_{n1}N_1 + A_{n2}N_2)\right]^{-1}, \quad (22)$$

with the initial concentrations of n_1 , n_2 and m_2 taken to be zero. The constants D and E appearing in equations (21) and (22) are given in appendix B. The numerical accuracy of the analytical expressions in this section is investigated in the next section.

3. Simulation—numerical results

We choose a set of numerical values for the parameters in the model from Pagonis *et al* [5]. These authors showed that the TL dose response of three different samples of $Al_2O_3:C$ could be described quantitatively by the model presented in this paper. The approach of Pagonis *et al* [5] was that the rate constants A_{n1}, A_{m1}, B_1, etc should be fixed constants for this material, but that the concentrations N_1, M_1, etc will vary from sample to sample.

The luminescence properties of the three samples termed Chip101, D320 and B1040 were studied extensively in Yukihara *et al* [9]. The values used for the present simulation are those obtained by Pagonis *et al* [5] for sample Chip101, and were based on the experimental data of Yukihara *et al* [9]. Specifically the values used in the simulations of this paper are $M_1 = 10^{17}\,\text{cm}^{-3}$; $M_2 = 2.4\times10^{16}\,\text{cm}^{-3}$; $N_1 = 2\times10^{15}\,\text{cm}^{-3}$; $N_2 = 2\times10^{15}\,\text{cm}^{-3}$; $A_{m1} = 4\times10^{-8}\,\text{cm}^3\,\text{s}^{-1}$; $A_{m2} = 5\times10^{-11}\,\text{cm}^3\,\text{s}^{-1}$; $B_1 = 10^{-8}\,\text{cm}^3\,\text{s}^{-1}$; $B_2 = 4\times10^{-9}\,\text{cm}^3\,\text{s}^{-1}$; $A_{n1} = 2\times10^{-8}\,\text{cm}^3\,\text{s}^{-1}$; $A_{n2} = 2\times10^{-9}\,\text{cm}^3\,\text{s}^{-1}$; $m_{10} = 9.4\times10^{15}\,\text{cm}^{-3}$ (Pagonis *et al* [5], table 1). The value of the irradiation dose rate is taken as $X = 1.7\times10^{15}\,\text{cm}^{-3}\,\text{s}^{-1}$ which was shown to correspond to a dose rate of $1\,\text{Gy}\,\text{s}^{-1}$ for this material (Chen *et al* [4]). The initial carrier concentrations in the model are taken equal to zero, except for the initial value m_{10} of the activated holes in the radiative centre. The chosen value of m_{10} for sample Chip101 corresponds to a 9.4% initial activation of the available recombination centres ($m_{10}/M_1 = 9.4\times10^{15}/10^{17} = 0.094$).

The simulation consists of two stages; firstly in the irradiation stage the differential equations (1)–(6) are solved for an irradiation time t_D. The RL intensity is simulated numerically by using equation (7). In the next stage of the simulation, a relaxation period has been simulated by setting the excitation dose rate $X = 0$ to zero, and solving the same set of equations for a short period of time so as to have the concentrations of the electrons, n_c, and free holes, n_v, go to negligible values. The initial values of the concentration functions for the relaxation stage are the final values at the excitation stage. In some of the simulations described later in this section these two stages are followed by a third stage, in which the sample is optically bleached for a few seconds in order to optically empty the optically active traps, as is done commonly experimentally between successive RL pulses.

Figure 3 depicts the simulated RL intensity $I(t)$ for a total irradiation time of 1 s, using the parameters of sample Chip101 and for several different values of the dose rate X in the range 0.1–0.5 $\text{Gy}\,\text{s}^{-1}$. The simulated RL signals in figure 3 are similar in shape to the experimentally measured RL signals from $Al_2O_3:C$ shown in figure 1(*a*). An initial short period in which the RL signal increases is followed by an approximately linear region, followed by a fast decreasing signal region. The solid lines through the simulated data points in figure 3 represent the analytical solutions given by the approximate equation (12) and with the constants C_1, C_2 given by equations (16)–(17). The agreement between the simulation results and the analytical expressions is very good for all times during the short irradiation pulses.

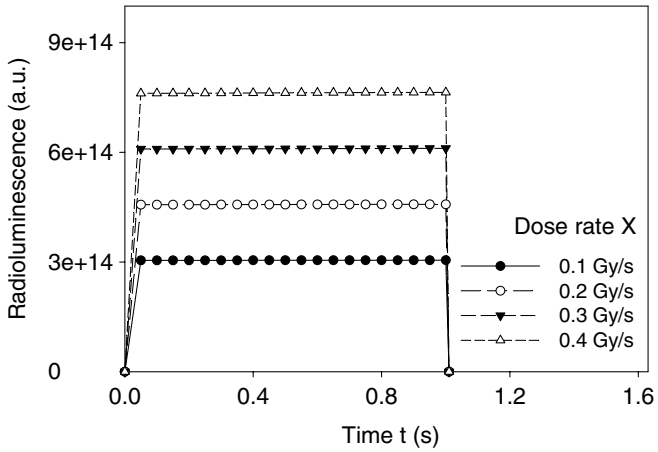

Figure 3. Simulated RL signal as a function of irradiation time t for several different values of the dose rate X. The relevant set of parameters is given in the text. The solid lines show the calculated RL signal using the analytical expression (12), (15) and (17). While the initial RL intensity increases linearly with the dose rate X, the slope of the linear part of the signal varies quadratically with the dose rate X.

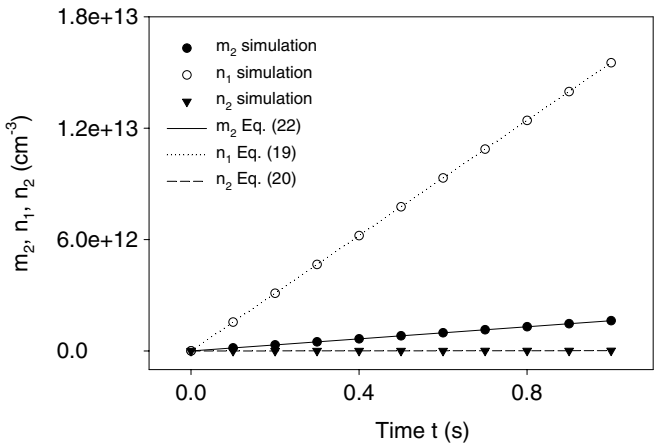

Figure 4. Simulated occupancies of the non-radiative centre m_2, of the dosimetric trap n_1 and of the competitor trap n_2, during the irradiation stage. All concentrations increase linearly during the irradiation stage. Also shown as solid lines are the calculated concentrations using the analytical expressions in the text.

Figures 4 and 5 depict the corresponding simulated occupancies of the non-radiative centre m_2, of the radiative centre m_1, of the dosimetric trap n_1 and of the competitor trap n_2, during the irradiation stage. The dose rate in figures 4 and 5 was 0.1 Gy s^{-1} and the duration of the RL pulse was 1 s. All four concentrations increase linearly during the irradiation stage. Also shown in figures 4 and 5 are the calculated concentrations using the analytical expressions in equations (19)–(22). The results in figures 4 and 5 show again good agreement between the simulated results obtained from the solution of the differential equations, and the approximate analytical expressions.

Figure 6 shows the simulated initial RL signal I_o from figure 3 plotted as a function of the dose rate X, yielding a linear dependence. This result is in agreement with the empirical dose rate dependence of the initial RL intensity

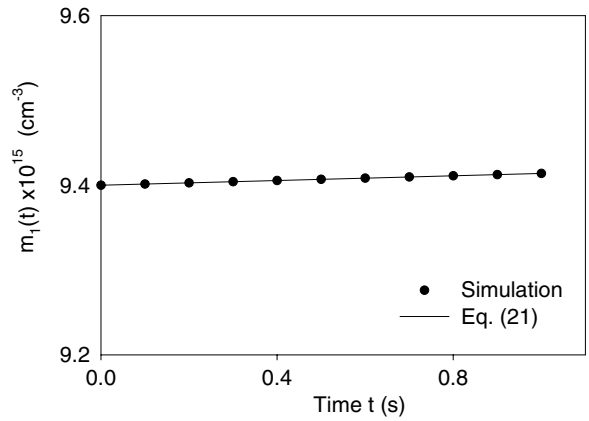

Figure 5. Simulated occupancy of the radiative centre m_1 during the irradiation stage, showing a linear increase with irradiation time. The solid line represents the calculated concentrations using the analytical equation (21) in the text. The initial concentration of radiative centre, $m_{10} = 9.4 \times 10^{17}$ cm^{-3}.

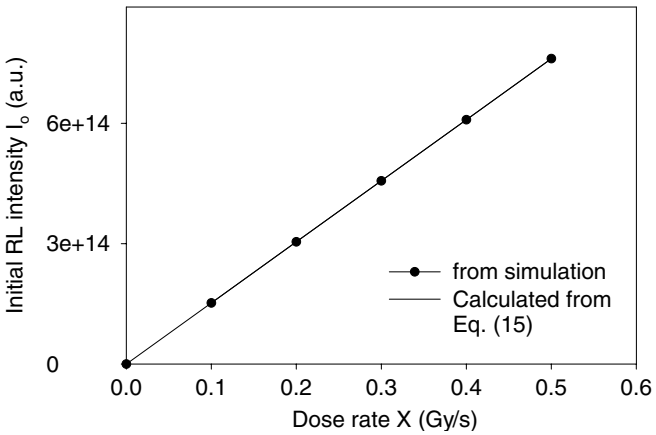

Figure 6. The initial RL signal I_o from figure 3 plotted as a function of the dose rate X, yielding a linear dependence. This result is in agreement with the empirical experimental data shown in figure 1(b), and with the exact analytical expression given in equation (15).

from $Al_2O_3:C$ shown in figure 1(b), and with the exact analytical expression given in equation (16). Figure 7 shows the simulated dependence of the slope of the linear part of the RL signal in figure 3, as a function of the square of the dose rate X^2. This dependence is again linear, as observed empirically previously in this material and as shown in the experimental data of figure 1(c). The linearity shown in figure 7 is in agreement with the analytical expression given in equation (17).

An important experimental consideration is whether the $Al_2O_3:C$ samples can be reused during a medical radiotherapy session. For example, the system developed by Andersen *et al* [1] provides *in vivo* measurements of the dose rate X during radiotherapy. Immediately after the treatment the CW OSL signal is used to determine the integrated dose, by optically bleaching the $Al_2O_3:C$ samples (see for example, Aznar *et al* [2]). We have simulated the delivery of 100 successive RL pulses, with each pulse followed by an optical bleach, with the simulated results shown in figure 8. As seen in figure 8 there is a very small change in the shape of the

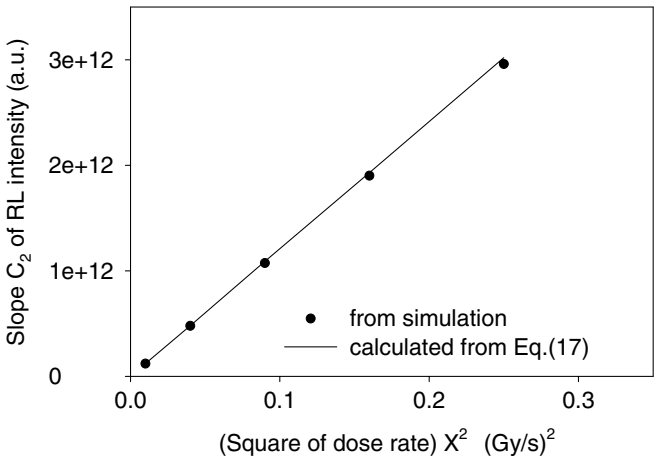

Figure 7. The slope of the linear part of the simulated RL signals in figure 3 is plotted as a function of the square of the dose rate X^2. This dependence is again linear, as observed empirically previously in this material and as shown in the experimental data of figure 1(*c*). The linearity shown in figure 7 is in agreement with the exact analytical expression given in equation (17).

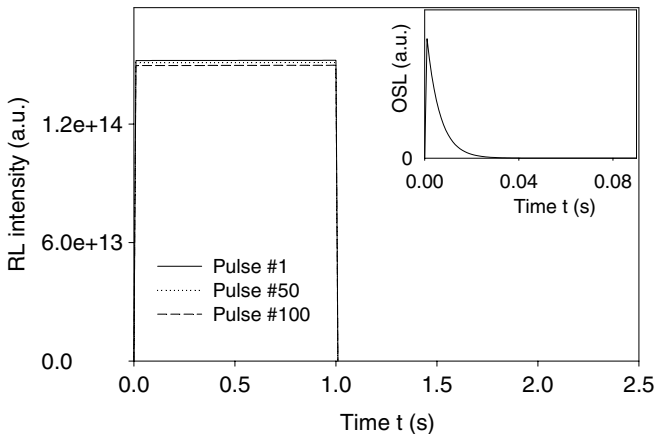

Figure 8. Simulation of 100 successive RL pulses with each pulse followed by an optical bleach of the sample. Each pulse corresponds to a dose of 0.1 Gy delivered at a dose rate of 0.1 Gy s^{-1}. The inset shows the simulated OSL signal obtained during the optical bleach after each RL pulse.

successive RL pulses, and even after 100 such pulses the RL intensity is changed by only a few per cent of its initial value.

Our main goal in this paper is to show that the analytical expressions can accurately describe the results of the simulation, rather than attempting to reproduce the exact experimental behaviour in figure 1(*a*). Nevertheless, it is possible to reproduce the experimental behaviour in figure 1(*a*) by modifying the initial concentration of holes in the recombination centre (m_{10}) in the model. Figure 9 shows the results of the simulation when using a much smaller value of $m_{10} = 4 \times 10^{13}\,\mathrm{cm}^{-3}$ in the model, while the rest of the parameters in the model were left unchanged. The dose rate in the simulation was adjusted so that the simulation results match the horizontal time-axis of the experimental data in figure 1(*a*). The simulated results for the RL intensity as a function of time shown in figure 9 compare well with the experimental behaviour in figure 1(*a*). The inset of figure 9 shows the corresponding time dependence $m_1(t)$ of the concentration of

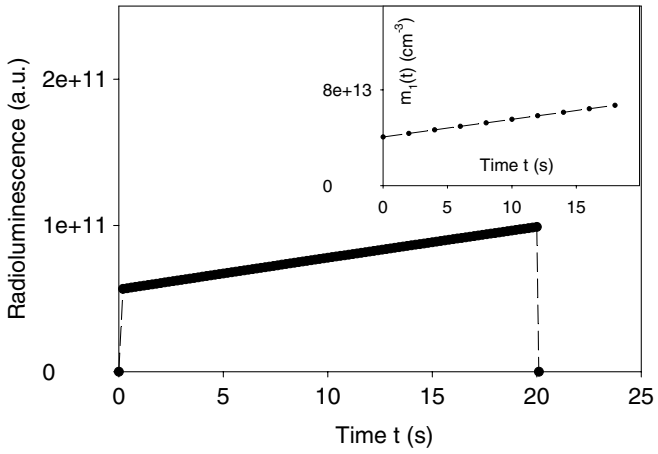

Figure 9. Simulation of the RL experiment using a much smaller initial value of $m_{10} = 4 \times 10^{13}\,\mathrm{cm}^{-3}$ in the model, while the rest of the parameters in the model were left unchanged. The simulated results for the RL intensity in this figure compare well with the experimental behaviour shown in figure 1(*a*). The inset shows the corresponding time dependence $m_1(t)$ of the concentration of holes in the recombination centre during irradiation. Both the concentration $m_1(t)$ and the RL intensity change by ∼40% during the short RL pulse.

holes in the recombination centre during irradiation, indicating an ∼40% change in both the concentration $m_1(t)$ and in the RL intensity.

Several previous experimental studies of this material [7, 9, 10] have shown that the non-radiative recombination centre (m_2) plays a critical role in determining the behaviour of this material during TL/OSL measurements. Within the RL simulations presented in this paper, this centre plays a rather minor role and serves as a weak competitor for the main radiative centre during irradiation. However, our previous simulations [4–6] have shown that this centre plays an important role in determining the non-monotonic dose behaviour of $Al_2O_3:C$.

4. Discussion–conclusions

The model presented in this paper can provide a quantitative description of RL signals from $Al_2O_3:C$. By assuming that the quasi-steady conditions hold, analytical expressions were derived for the concentration of traps and centres during sample irradiation with short pulses. The numerical solutions of the differential equations are found to be in close agreement with the derived analytical expressions for short irradiation pulses.

Several previously reported empirical results are explained within the model. Previously, the linear dependence of the initial RL intensity I_o on the dose rate X was interpreted as due to sensitivity changes taking place in the material during irradiation. Specifically, a possible explanation was offered by Polf *et al* [10], who describe a similar increase in the RL intensity and state that 'in a general model, an increase in the RL is expected with the filling of all electron traps, including shallow and deep electron traps, as the trapping probability decreases and more electrons become available for recombination'. The results presented in this paper show that at least

within the range of parameters used in our model, this linear dependence of I_o on the dose rate X is actually due to the increase in the concentration of holes (m_1) in the radiative recombination centre during irradiation. This increase leads to an apparent change in the RL sensitivity of the sample, as seen in figures 5 and 9. This previous empirical experimental result has now been given an analytical description in this paper, in the form of equation (21).

However, it is quite possible that in a different sample of this material, in which the traps and centres are closer to saturation, the experimentally observed sensitivity change is caused by the filling of the traps and centres as saturation is approached.

The empirically observed linear dependence of the slope of the RL intensity on the square of the dose rate X^2 was expressed analytically in equation (17) and is in close agreement with the numerical results from the model.

This paper also presents the results of simulations in which several successive pulses are followed by optical bleaching, to test whether the shape and intensity of RL pulses change between successive uses of the same $Al_2O_3:C$ samples in medical dosimetry. The results of the simulations show that at least within the kinetic parameters presented in this paper for sample D320, there is very small change in the shape and intensity of the successive RL pulses, and therefore it should be possible to reuse the same optical fibres several times during medical dosimetry.

Appendix A: derivation of the coefficient C_2 for the RL intensity $I(t)$

In this appendix we derive a rigorous general expression for the RL intensity $I(t)$. The only assumptions used during this derivation are that the quasi-steady conditions hold and that the initial concentrations of electrons and holes in the model are $m_1(0) = m_{10}$ and $n_{10} = n_{20} = m_{20} = 0$. Due to the complex nature of the algebra involved, the derivation of several algebraic expressions in the two appendices were checked using the symbolic manipulation capability of the package *Mathematica*.

For short irradiation pulses the RL intensity $I(t)$ can be expanded as a Taylor series about $t = 0$. Our goal is to find the first two terms of the series expansion:

$$I(t) = C_1 + C_2 t + O(t^2), \tag{23}$$

with the coefficients C_1 and C_2 given by

$$C_1 = I(0), \tag{24}$$

$$C_2 = \left.\frac{\mathrm{d}I(t)}{\mathrm{d}t}\right|_{t=0}. \tag{25}$$

In order to calculate the constant C_2 we proceed as follows:

$$C_2 = \left.\frac{\mathrm{d}I(\mathrm{t})}{\mathrm{d}t}\right|_{t=0} = \left.\frac{\mathrm{d}(A_{m1}m_1n_\mathrm{c})}{\mathrm{d}t}\right|_{t=0} = A_{m1}\left.\frac{\mathrm{d}(m_1n_\mathrm{c})}{\mathrm{d}t}\right|_{t=0}$$
$$= A_{m1}\left[n_\mathrm{c}\frac{\mathrm{d}m_1}{\mathrm{d}t} + m_1\frac{\mathrm{d}n_\mathrm{c}}{\mathrm{d}t}\right]_{t=0}. \tag{26}$$

Substituting the exact value of n_c from equation (10) into equation (26) we obtain

$$C_2 = A_{m1}\left[n_\mathrm{c}\frac{\mathrm{d}m_1}{\mathrm{d}t} + m_1\frac{\mathrm{d}}{\mathrm{d}t}\left(\frac{X}{A_{n1}(N_1-n_1)+A_{n2}(N_2-n_2)+A_{m1}m_1+A_{m2}m_2}\right)\right]_{t=0}. \tag{27}$$

After differentiating,

$$C_2 = A_{m1}\left[n_\mathrm{c}\frac{\mathrm{d}m_1}{\mathrm{d}t} + m_1X\left(\frac{A_{n1}\frac{\mathrm{d}n_1}{\mathrm{d}t} + A_{n2}\frac{\mathrm{d}n_2}{\mathrm{d}t} - A_{m1}\frac{\mathrm{d}m_1}{\mathrm{d}t} - A_{m2}\frac{\mathrm{d}m_2}{\mathrm{d}t}}{(A_{n1}(N_1-n_1) + A_{n2}(N_2-n_2) + A_{m1}m_{10})^2}\right)\right]_{t=0}. \tag{28}$$

To replace the denominator in equation (28) we can use equation (10) again to obtain

$$C_2 = A_{m1}\left[n_\mathrm{c}\frac{\mathrm{d}m_1}{\mathrm{d}t} + \frac{m_1n_\mathrm{c}^2}{X}\left(A_{n1}\frac{\mathrm{d}n_1}{\mathrm{d}t} + A_{n2}\frac{\mathrm{d}n_2}{\mathrm{d}t} - A_{m1}\frac{\mathrm{d}m_1}{\mathrm{d}t} - A_{m2}\frac{\mathrm{d}m_2}{\mathrm{d}t}\right)\right]_{t=0}. \tag{29}$$

Collecting the $\frac{\mathrm{d}m_1}{\mathrm{d}t}$ terms:

$$C_2 = \frac{A_{m1}n_\mathrm{c}(0)}{X}\left[(X - A_{m1}m_1n_\mathrm{c})\frac{\mathrm{d}m_1}{\mathrm{d}t} + m_1n_\mathrm{c}\left(A_{n1}\frac{\mathrm{d}n_1}{\mathrm{d}t} + A_{n2}\frac{\mathrm{d}n_2}{\mathrm{d}t} - A_{m2}\frac{\mathrm{d}m_2}{\mathrm{d}t}\right)\right]_{t=0}. \tag{30}$$

Substituting the values of the derivatives from equations (1) through (4) in (30) gives

$$C_2 = \frac{A_{m1}n_\mathrm{c}(0)}{X}[(X - A_{m1}m_1n_\mathrm{c})(B_1(M_1 - m_1)n_\mathrm{v} - A_{m1}m_1n_\mathrm{c}) + m_1n_\mathrm{c}(A_{n1}^2(N_1 - n_1)n_\mathrm{c} + A_{n2}^2(N_2 - n_2)n_\mathrm{c} - A_{m2}B_2(M_2 - m_2)n_\mathrm{v} + A_{m2}^2m_2n_\mathrm{c})]_{t=0}. \tag{31}$$

We can now evaluate all the terms in (31) at time $t = 0$:

$$C_2 = \frac{A_{m1}n_{\mathrm{c}0}}{X}[(X - A_{m1}m_{10}n_{\mathrm{c}0})(B_1(M_1 - m_{10})n_{\mathrm{v}0} - A_{m1}m_{10}n_\mathrm{c}0) + m_{10}n_{\mathrm{c}0}(A_{n1}^2N_1n_{\mathrm{c}0} + A_{n2}^2N_2n_{\mathrm{c}0} - A_{m2}B_2M_2n_{\mathrm{v}0})]. \tag{32}$$

Rearranging to factor out another n_c term yields

$$C_2 = \frac{A_{m1}n_{\mathrm{c}0}^2}{X}\left[\left(\frac{X}{n_{\mathrm{c}0}} - A_{m1}m_{10}\right)(B_1(M_1 - m_{10})n_{\mathrm{v}0} - A_{m1}m_{10}n_{\mathrm{c}0}) + m_{10}(A_{n1}^2N_1n_{\mathrm{c}0} + A_{n2}^2N_2n_{\mathrm{c}0} - A_{m2}B_2M_2n_{\mathrm{v}0})\right]. \tag{33}$$

From equation (10) we know that $(X/n_{c0}) - A_{m1}m_{10} = A_{n1}N_1 + A_{n2}N_2$, so we can write

$$C_2 = \frac{A_{m1}n_{c0}^2}{X}[(A_{n1}N_1 + A_{n2}N_2)(B_1(M_1 - m_{10})n_{v0} - A_{m1}m_{10}n_{c0}) + m_{10}(A_{n1}^2N_1n_{c0} + A_{n2}^2N_2n_{c0} - A_{m2}B_2M_2n_{v0})]. \quad (34)$$

Rearranging to collect together terms involving n_{c0} and terms involving n_{v0} yields

$$C_2 = \frac{A_{m1}n_{c0}^2}{X}[n_{c0}m_{10}(A_{n1}^2N_1 + A_{n2}^2N_2 - A_{m1}(A_{n1}N_1 + A_{n2}N_2)) + n_{v0}((A_{n1}N_1 + A_{n2}N_2)B_1(M_1 - m_{10}) - A_{m2}B_2M_2m_{10})]. \quad (35)$$

Now substituting the quasi-steady values of n_{c0} and n_{v0} from equations (9) and (11) yields the desired exact expression for the constant C_2:

$$C_2 = \frac{A_{m1}X^2}{(A_{n1}N_1 + A_{n2}N_2 + A_{m1}m_{10})^2} \times\left(m_{10}\frac{A_{n1}^2N_1 + A_{n2}^2N_2 - A_{m1}(A_{n1}N_1 + A_{n2}N_2)}{A_{n1}N_1 + A_{n2}N_2 + A_{m1}m_{10}} + \frac{(A_{n1}N_1 + A_{n2}N_2)B_1(M_1 - m_{10}) - A_{m2}B_2M_2m_{10}}{B_1(M_1 - m_{10}) + B_2M_2}\right). \quad (36)$$

This is the result quoted in equation (17).

Appendix B: calculation of the concentrations $m_1(t)$, $m_2(t)$, $n_1(t)$, $n_2(t)$

By substituting equations (9) and (11) into equation (1) we obtain

$$\frac{dm_1}{dt} = -A_{m1}m_1n_c + B_1(M_1 - m_1)n_v = -A_{m1}m_1\frac{X}{A_{n1}N_1 + A_{n2}N_2 + A_{m1}m_{10}} + B_1(M_1 - m_1)\frac{X}{B_2M_2 + B_1(M_1 - m_{10})} \quad (37)$$

This is a first order differential equation for $m_1(t)$ with the initial condition $m_1(0) = m_{10}$. and its solution is obtained using standard integration methods to yield

$$m_1(t) = \left[A_{m1}m_{10}(B_1M_1 + B_2M_2e^{-DtX}) + B_1(M_1(1 - e^{-DtX}) + m_{10})(A_{n1}N_1 + A_{n2}N_2)\right] \times\left[A_{m1}B_1M_1 + A_{m1}B_2M_2 + A_{n1}B_1N_1 + A_{n2}B_1N_2\right]^{-1}, \quad (38)$$

with the constant D equal to

$$D = \frac{A_{m1}B_1M_1 + A_{m1}B_2M_2 + A_{n1}B_1N_1 + A_{n2}B_1N_2}{(B_1M_1 - B_1m_{10} + B_2M_2)(A_{m1}m_{10} + A_{n1}N_1 + A_{n2}N_2)}. \quad (39)$$

Equation (38) indicates that the concentration of holes in the radiative centre increases with time, in the form of a saturating increasing exponential function. The limit of this equation as $t \to 0$ is $m_1(t) \to m_{10}$, as may be expected on physical grounds. The limit of $m_1(t)$ for very large times $t \to \infty$ is a finite value which depends on the numerical values of the parameters in the model.

In a similar manner we can obtain the desired expression of the concentration $m_2(t)$ of the non-radiative centre, by substituting equations (9) and (11) into equation (2) to obtain

$$\frac{dm_2}{dt} = -A_{m2}m_2n_c + B_2(M_2 - m_2)n_v = -A_{m2}m_2\frac{X}{A_{n1}N_1 + A_{n2}N_2 + A_{m1}m_{10}} + B_2(M_2 - m_2)\frac{X}{B_2M_2 + B_1(M_1 - m_{10})}. \quad (40)$$

This is again a first order differential equation for $m_2(t)$ with the initial condition $m_{20} = 0$. Its solution is

$$m_2(t) = \left[B_2M_2(1 - e^{-EtX})(A_{n1}N_1 + A_{n2}N_2 + A_{m1}m_{10})\right] \times\left[A_{m2}(B_1M_1 - B_1m_{10} + B_2M_2) + B_2(A_{m1}m_{10} + A_{n1}N_1 + A_{n2}N_2)\right]^{-1}. \quad (41)$$

With the constant E given by the expression

$$E = \left[A_{m2}(B_1M_1 - B_1m_{10} + B_2M_2) + B_2(A_{m1}m_{10} + A_{n1}N_1 + A_{n2}N_2)\right] \times\left[(B_1M_1 - B_1m_{10} + B_2M_2)(A_{m1}m_{10} + A_{n1}N_1 + A_{n2}N_2)\right]^{-1}. \quad (42)$$

Equation (41) indicates that the concentration of holes in the non-radiative centre also increases with time, in the form of a saturating increasing exponential function. The limit of this equation as $t \to 0$ is $m_2(t) \to 0$. The limit of $m_2(t)$ for very large times $t \to \infty$ is a finite value which depends on the value of the parameters in the model.

In a similar manner we obtain the following analytical expressions for the concentrations of electrons n_1, n_2 in the dosimetric trap and in the deep electron trap correspondingly:

$$n_1(t) = N_1\left(1 - \exp\left(-\frac{A_{n1}Xt}{A_{n2}N_2 + A_{n1}N_1 + A_{m1}m_{10}}\right)\right), \quad (43)$$

$$n_2(t) = N_2\left(1 - \exp\left(-\frac{A_{n2}Xt}{A_{n2}N_2 + A_{n1}N_1 + A_{m1}m_{10}}\right)\right). \quad (44)$$

Equations (43) and (44) indicate that the electron concentrations in the dosimetric trap (n_1) and in the deep electron trap (n_2) increase continuously with irradiation time during a RL experiment, in the form of saturating exponential functions.

For short irradiation times such that $(A_{n1}Xt/A_{n1}N_1 + A_{n2}N_2 + A_{m1}m_{10}) \ll 1$, the exponential in expression (43) can be approximated with a linear function $n_1(t)$, as shown in the simulation results of figure 4. Similar conditions for the time t corresponding to short irradiation pulses can be obtained for $m_1(t)$, $m_2(t)$ and $n_2(t)$ from equations (38), (41) and (44) correspondingly.

References

[1] Andersen C E, Marckmann C J, Aznar M C, Bøtter-Jensen L, Kjær-Kristoffersen F and Medin J 2006 *Radiat. Prot. Dosim.* **120** 7–13

[2] Aznar M C, Andersen C E, Bøtter-Jensen L, Bäck S Å J, Mattson S, Kjær-Kristoffersen F and Medin J 2004 *Phys. Med. Biol.* **49** 1655–69

[3] Aznar M C 2005 Real-time in vivo luminescence dosimetry in radiotherapy and mammography using $Al_2O_3:C$ *PhD Thesis* p134 Risø-PhD-12(EN) Available online at http://www.risoe.dtu.dk/rispubl/NUK/nukpdf/ris-phd-12.pdf

[4] Chen R, Pagonis V and Lawless J L 2006 *J. Appl. Phys.* **99** 033511

[5] Pagonis V, Chen R and Lawless J L 2007 *Radiat. Meas.* **42** 198–204

[6] Pagonis V, Chen R and Lawless J L 2008 *Radiat. Meas.* **43** 175–9

[7] Akselrod M S, Bøtter-Jensen L and McKeever S W S 2006 *Radiat. Meas.* **41** S78–99

[8] Edmund J M and Andersen C E 2007 *Radiat. Meas.* **42** 177–89

[9] Yukihara E G, Whitley V H, Polf J C, Klein D M, McKeever S W S, Akselrod A E and Akselrod M S 2003 *Radiat. Meas.* **37** 627–38

[10] Polf J C, Yukihara E G, Akselrod M S and McKeever S M S 2004 *Radiat. Meas.* **38** 227–40

[11] Trautmann T 2000 *J. Phys. D: Appl. Phys.* **33** 2304–10

[12] Trautmann T, Krbetschek M R, Dietrich A and Stolz W 2000 *Radiat. Meas.* **32** 487–92

[13] Trautmann T, Krbetschek M R, Dietrich A and Stolz W 1998 *Radiat. Meas.* **29** 421–5

[14] McKeever S W S and Chen R 1997 *Radiat. Meas.* **27** 625–61

[15] McKeever S W S, Agersnap Larsen N, Bøtter-Jensen L and Mejdahl V 1997 *Radiat. Meas.* **27** 75–82